



## RESEARCH LETTER

10.1002/2016GL072319

## Key Points:

- We hypothesize that viscous flow significantly modifies cryovolcanic structures on Ceres
- We find that cryovolcanoes on Ceres are modified on  $10^7$ – $10^9$  year timescales if they are >40% ice by volume
- Viscous relaxation as a modification mechanism is consistent with cryovolcanism occurring throughout Cerean history

## Supporting Information:

- Supporting Information S1

## Correspondence to:

M. M. Sori,  
michael.sori@gmail.com

## Citation:

Sori, M. M., S. Byrne, M. T. Bland, A. M. Bramson, A. I. Ermakov, C. W. Hamilton, K. A. Otto, O. Ruesch, and C. T. Russell (2017), The vanishing cryovolcanoes of Ceres, *Geophys. Res. Lett.*, *44*, 1243–1250, doi:10.1002/2016GL072319.

Received 13 DEC 2016

Accepted 20 JAN 2017

Accepted article online 24 JAN 2017

Published online 10 FEB 2017

## The vanishing cryovolcanoes of Ceres

Michael M. Sori<sup>1</sup> , Shane Byrne<sup>1</sup> , Michael T. Bland<sup>2</sup>, Ali M. Bramson<sup>1</sup> , Anton I. Ermakov<sup>3</sup> , Christopher W. Hamilton<sup>1</sup> , Katharina A. Otto<sup>4</sup> , Ottaviano Ruesch<sup>5</sup>, and Christopher T. Russell<sup>6</sup> 

<sup>1</sup>Lunar and Planetary Laboratory, University of Arizona, Tucson, Arizona, USA, <sup>2</sup>U. S. Geological Survey Astrogeology Science Center, Flagstaff, Arizona, USA, <sup>3</sup>Jet Propulsion Laboratory, California Institute of Technology, Pasadena, California, USA, <sup>4</sup>German Aerospace Center (DLR), Berlin, Germany, <sup>5</sup>NASA Goddard Space Flight Center/Universities Space Research Association, Greenbelt, Maryland, USA, <sup>6</sup>Earth Planetary and Space Sciences, University of California, Los Angeles, California, USA

**Abstract** Ahuna Mons is a 4 km tall mountain on Ceres interpreted as a geologically young cryovolcanic dome. Other possible cryovolcanic features are more ambiguous, implying that cryovolcanism is only a recent phenomenon or that other cryovolcanic structures have been modified beyond easy identification. We test the hypothesis that Cerean cryovolcanic domes viscously relax, precluding ancient domes from recognition. We use numerical models to predict flow velocities of Ahuna Mons to be 10–500 m/Myr, depending upon assumptions about ice content, rheology, grain size, and thermal parameters. Slower flow rates in this range are sufficiently fast to induce extensive relaxation of cryovolcanic structures over  $10^8$ – $10^9$  years, but gradual enough for Ahuna Mons to remain identifiable today. Positive topographic features, including a tholus underlying Ahuna Mons, may represent relaxed cryovolcanic structures. A composition for Ahuna Mons of >40% ice explains the observed distribution of cryovolcanic structures because viscous relaxation renders old cryovolcanoes unrecognizable.

## 1. Introduction

NASA's Dawn mission [Russell et al., 2016] observed Ahuna Mons (Figure 1), a 4 km high landform on Ceres interpreted to be a cryovolcanic dome [Ruesch et al., 2016a]. Cryovolcanism is a form of volcanism involving water or other volatiles instead of silicate magmas [e.g., Kargel, 1991]. Cryovolcanic domes have been proposed on numerous bodies including Titan [Lopes et al., 2007], Europa [Quick et al., 2017], and Pluto [Moore et al., 2016], and Ahuna Mons represents one of the best examples of such a construct. Ruesch et al. [2016a] argued that Ahuna Mons is a cryovolcanic structure on the basis of morphology and models of emplacement processes. A tectonic origin was ruled out based on a lack of observed compressional features, and diapirism was ruled out based on the lack of evidence for a thin, elastic layer [Ruesch et al., 2016a]. Key morphological characteristics in support of the cryovolcanic origin of Ahuna Mons include fractures on the summit and an aspect ratio (height/average basal diameter) of  $\sim 0.24$ , which is similar to some terrestrial volcanic domes [Fink and Bridges, 1995]. Ruesch et al. [2016a] hypothesize that steep ( $30^\circ$ – $40^\circ$ ) flanks, near the angle of repose, represent a talus unit accumulated from fracturing of a brittle carapace during the cryovolcanic emplacement process. A positive Bouguer gravity anomaly exists in the region [Ermakov et al., 2016a]. Because of the nonuniqueness of gravity solutions, this anomaly could have a number of causes; one possible cause is a thin crust which may make the region favorable for cryovolcanism sourced from beneath the crust. A cryovolcanic origin has also been suggested for flow features found in some craters on Ceres [Krohn et al., 2016].

Analyses of the crater size-frequency distributions of geologic units underlying Ahuna Mons constrain the cryovolcanic activity to be at most  $210 \pm 30$  or  $70 \pm 20$  Myr old, depending on the crater production function used [Hiesinger et al., 2016; Ruesch et al., 2016a]. These estimates are geologically young, leading to the question of why other prominent cryovolcanic structures are not observed on Ceres. Assuming that cryovolcanism on Ceres is not a new phenomenon, there must be some process that destroys or obscures older cryovolcanic landforms. Collapse of terrestrial volcanic domes is common [Voight and Elsworth, 1997], but there is no observational evidence for such a process occurring on Ceres.

We hypothesize that viscous relaxation, which is known to shape the surfaces of some planetary bodies, is responsible for modifying cryovolcanic domes. Viscous deformation is unlikely to perfectly erase topography on Ceres into a level plain but may modify landforms sufficiently such that they are difficult to

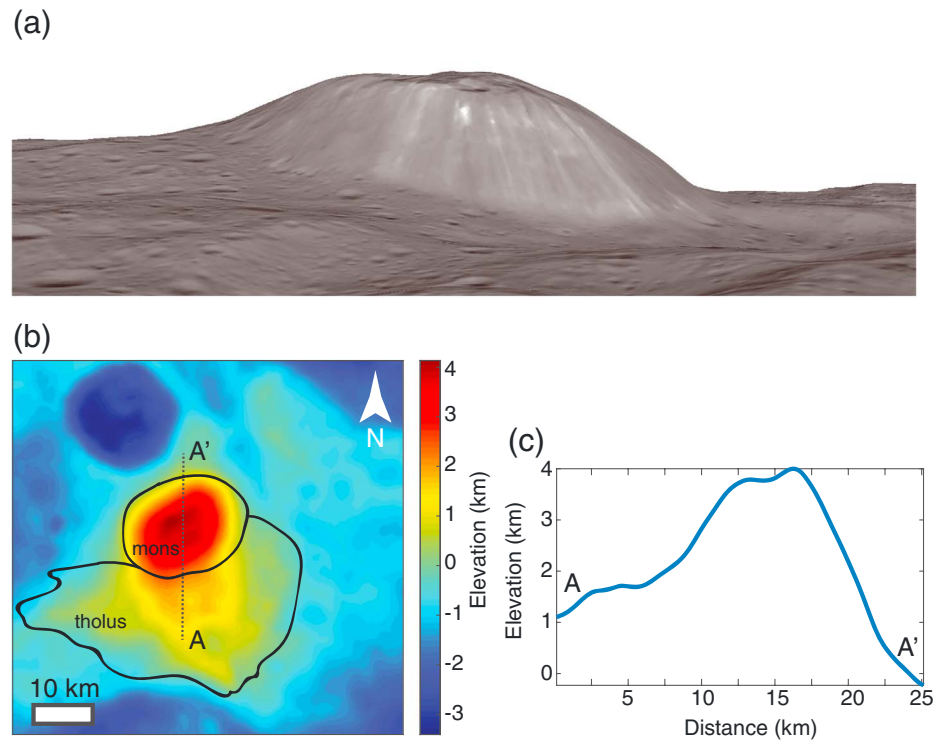


**Figure 1.** (a) Simulated west facing perspective view of  $\sim 17$  km wide Ahuna Mons ( $10.3^{\circ}\text{S}$ ,  $316.2^{\circ}\text{E}$ ) from Dawn Framing Camera stereo images. (b) Topography (relative to a  $482 \times 482 \times 446$  km reference ellipsoid) from Dawn stereophotogrammetry, with Ahuna Mons and tholus unit (discussed in section 4) outlined with solid black lines. (c) N-S topographic profile across Ahuna Mons represented by dotted line in Figure 1b.

identify. This mechanism requires structures to be sufficiently ice rich to flow. High crater density, especially at relatively warm low latitudes, reveals that the Cerean crust is not sufficiently ice rich to smooth out topography at the kilometer or tens of kilometers scale everywhere on the surface [Bland, 2013]. This observation is consistent with Dawn geophysical observations [Ermakov *et al.*, 2016a; Fu *et al.*, 2016; Park *et al.*, 2016], which reveal that Ceres (whose bulk density suggests an ice-rock mixture) is only partially differentiated [Zolotov, 2009] into icy and rocky layers in contrast to some pre-Dawn predictions of complete differentiation [McCord and Sotin, 2005; Thomas *et al.*, 2005; Castillo-Rogez and McCord, 2010; Castillo-Rogez, 2011]. However, while the crust on average must be  $<30\%$  ice by volume to support topography [Fu *et al.*, 2016], variation in crater morphology [Bland *et al.*, 2016] and spectroscopic detection of localized  $\text{H}_2\text{O}$  [Combe *et al.*, 2016] indicate that ice content is laterally heterogeneous. Localized regions or individual landforms may be sufficiently ice rich for flow to occur [Schmidt *et al.*, 2016] even if the crust as a whole is not.

Cryovolcanic domes are viable candidate landforms to be anomalously ice rich because they are sourced from parental magmas that include water [Ruesch *et al.*, 2016a]. Viscous flow could thus be an important mechanism in their evolution postemplacement. The viscosity of water ice is much lower than that of silicate rock, so this mechanism has no analogy on silicate volcanoes. Viscous relaxation may be the dominant modification mechanism for Cerean cryovolcanoes.

In this paper, we study the viscous evolution of postemplacement cryovolcanic structures on Ceres and estimate flow velocities of Ahuna Mons throughout geologic time. Our methodology is similar to techniques used to quantify potential viscous relaxation of other icy geologic landforms, including dome-like features on Europa [Miyamoto *et al.*, 2005], troughs and cliffs at the Martian polar caps [Pathare and Paige, 2005; Sori *et al.*, 2016], and craters on icy satellites [Dombard and McKinnon, 2006; Bland *et al.*, 2012]. We test the robustness of our results to various input parameters that are only moderately constrained for Ceres. We discuss the implications of our results for Cerean cryovolcanic history.

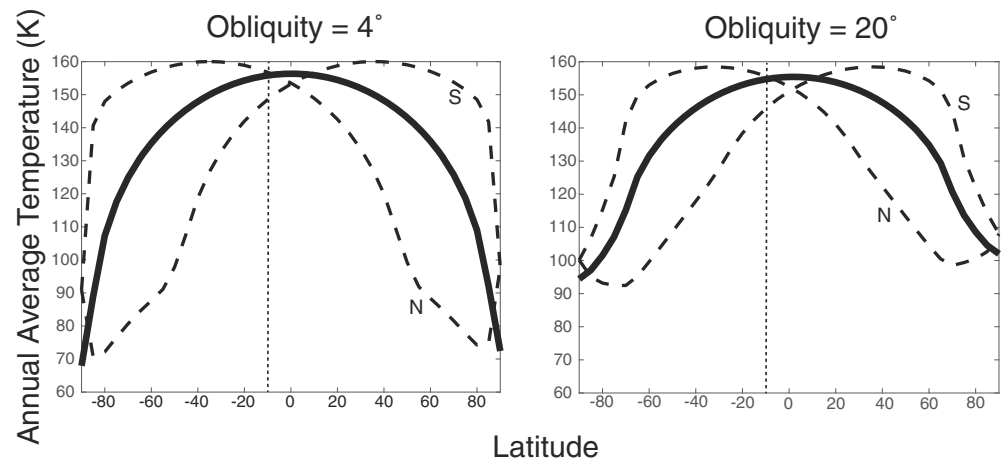


**Figure 2.** Thermal model results showing annual-average temperatures as a function of latitude at Ceres' (left) current obliquity, which is very near its minimum obliquity, and (right) maximum obliquity. Solid lines represent results for flat topography, dashed lines represent results for north (labeled N) and south (labeled S) facing 40° slopes. Vertical dotted line represents location of Ahuna Mons.

## 2. Thermal Model

Ice flow models are sensitive to temperature because it has a large effect on ice viscosity [e.g., Glen, 1955]. As such, we simulate temperatures of Cerean mountains, treating them as an ice-silicate mixture. Material properties may change with depth; we assume that there is consolidated ice-silicate material beneath low thermal inertia regolith. We use our resulting temperatures as input to our flow models. We estimate the annual-average temperature on Ceres as a function of latitude using a 1-D semi-implicit thermal model that simulates energy balance at the surface from insolation, blackbody radiation, and thermal conduction with subsurface layers. We solve the thermal diffusion equation at the boundaries of subsurface layers. We use 15 layers within one diurnal skin depth, with layer thickness increasing by 3% until six annual skin depths are reached. At the surface, we balance incoming and outgoing radiation with conduction to the subsurface. We use a zero flux lower boundary condition; Ceres' maximum heat flux is  $1 \text{ mW/m}^2$  [Castillo-Rogez et al., 2016], which increases flow velocities by  $<1\%$  compared to zero flux. For our nominal case, we assume current Cerean orbital parameters in order to calculate solar fluxes at each latitude. At the surface, we assume an albedo of 0.1, an infrared emissivity of 0.9, and a thermal inertia of  $15 \text{ J m}^{-2} \text{ s}^{-0.5} \text{ K}^{-1}$  [Hayne and Aharonson, 2015]. We choose the global average albedo so our results are generally applicable to Ceres, but the relatively bright albedo of Ahuna Mons decreases annual-average temperatures by  $<0.5 \text{ K}$ . Our nominal temperatures for Ahuna Mons are calculated under the assumption that consolidated material lies beneath 1 cm thick regolith, but we find that increasing regolith thickness to 5 cm affects annual-average temperatures by  $<1 \text{ K}$ . A table of parameters used in the thermal model can be found in the supporting information (Table S1).

Our thermal models, which calculate temperature every 500 s, yield annual-average temperatures for flat topography on Ceres that range from 66 to 159 K (Figure 2), consistent with Dawn data and previous modeling results [Hayne and Aharonson, 2015]. Ahuna Mons is near the warmest part of that range due to its low latitude ( $\sim 10^\circ\text{S}$ ). We calculate the annual thermal skin depth to be approximately tens of centimeters, justifying the use of annual-average temperatures for  $\sim 4 \text{ km}$  tall Ahuna Mons and similarly sized features. The interior was likely warmer immediately after emplacement; the conductive timescale of an object of this size and composition is of order  $10^5$  years [Ruesch et al., 2016a], so our modeling is applicable after that initial period.

We consider the effects of surface slope. The slopes of Ahuna Mons are as high as  $\sim 40^\circ$ , near the angle of repose. As end-members, we calculate temperatures of equatorward and poleward facing  $40^\circ$  slopes at every latitude. Sloped terrain experiences different insolation because slopes change the angle of incidence and also cause part of the sky to be obstructed by surrounding terrain. We estimate this effect by modeling the flat surrounding surface independently [e.g., Aharonson and Schorghofer, 2006] and adding thermal emission and visible-light reflection toward the slope to direct solar radiation. We find that the annual-average

temperature of sloped terrain differs by a few kelvins from flat terrain at Ahuna Mons' location and other low latitudes, but this effect increases at the midlatitudes with a maximum difference at  $\sim 55^\circ\text{S}$  (Figure 2).

We consider the effects of Ceres' varying obliquity. Ceres is currently at an obliquity of  $\sim 4^\circ$ , but this is near its minimum. Ceres undergoes obliquity variations with a  $\sim 24,500$  year periodicity and a maximum obliquity of  $\sim 20^\circ$  [Bills and Scott, 2017; Ermakov et al., 2016b]. We ran the same thermal model at this maximum obliquity and found that annual-average temperatures vary by  $< 2$  K between Ceres' minimum and maximum obliquities at latitudes  $< 60^\circ$  and by 1 K at Ahuna Mons' location (Figure 2). Therefore, obliquity variations only become important near the poles, and we use the current obliquity in our flow simulations.

### 3. Flow Model

We use the software Elmer/Ice [Gagliardini et al., 2013], a finite element method (FEM) code developed for terrestrial ice dynamics problems. We solve the Stokes equations for conservation of linear mass and momentum, adapting Elmer/Ice for our specific planetary context by changing surface gravity and inputting temperatures from our thermal simulations.

For rheology, we use the laws of Goldsby and Kohlstedt [2001], which separate strain rate into various deformation mechanisms (effects of choosing this rheology instead of Glen [1955] are discussed later). For the temperatures and deviatoric stresses applicable within Ahuna Mons (calculated in Elmer/Ice to be 0.1–1.0 MPa), we find diffusion creep to be negligible and basal slip to be limited by grain boundary sliding. The controlling deformation mechanisms are dislocation creep (where individual ice crystals are deformed by the movement of irregularities through the crystal structure [Durham et al., 1992]) and grain boundary sliding (where whole grains slide past one another [Goldsby and Kohlstedt, 2001]). The strain rates for these two deformation mechanisms are given, respectively, by

$$\dot{\epsilon}_{\text{dis}} = \frac{3^{2.5}}{2} \times 400,000 e^{-8\phi - \frac{60,000}{RT}} \tau^4 \quad (1)$$

$$\dot{\epsilon}_{\text{GBS}} = \frac{3^{1.4}}{2} \times 0.0039 e^{-3.6\phi - \frac{40,000}{RT}} \tau^{1.8} d^{-1.4} \quad (2)$$

$R$  is the gas constant,  $T$  is temperature in K,  $\tau$  is deviatoric stress in MPa,  $\phi$  is silicate volume fraction, and  $d$  is ice grain size in meters. The two strain rates are summed for the total strain rate [Goldsby and Kohlstedt, 2001]. Equations (1) and (2) are applicable for temperatures  $< 250$  K, which our thermal model results show is appropriate for Ceres. A table of parameters used in the flow model can be found in the supporting information (Table S2).

We ran FEM simulations of Ahuna Mons in 3-D. We approximate Ahuna Mons as a 4 km high truncated cone with a flat top and an ellipsoidal base (axes 21 km and 13 km [Ruesch et al., 2016a]) and  $40^\circ$  slopes. We assume that the underlying topography is planar and immobile compared to ice-rich features [Fu et al., 2016; Ermakov et al., 2016a]; therefore, the thickness of the underlying crust has no effect on our results. The presence of an underlying tholus unit (see section 4) will not affect flow velocities even if it has similar composition to Ahuna Mons. We assume that Ahuna Mons' base is frozen to the underlying topography because of low temperatures; therefore, our boundary conditions are a free surface for the top surface of our model with no sliding at the base. We mesh the domain with nodes every 100 m and find that our resultant flow velocities do not significantly change with increasing node density. Ice grain size and rock volume fraction are not well constrained but decrease strain rates with increasing values [Goldsby and Kohlstedt, 2001; Durham and Stern, 2001] according to equations (1) and (2); we take them as free parameters. Based on our thermal model results, our nominal case is run at 155 K (a uniform temperature is allowable because of the low latitude, Figure 2), but we run simulations at other temperatures, including nonuniform temperature distributions for different slope aspects, in order to apply our results to other hypothetical cryovolcanic domes at different latitudes.

Instantaneous flow velocities are shown for Ahuna Mons in Figure 3. As expected, mass flows outward and downward, shallowing the mountain's slopes over time. We consider a case where Ahuna Mons is composed of pure ice. While a lack of ice detection at the surface of Ahuna Mons [Zambon et al., 2016] does not preclude the possibility that most of the volume is icy, a pure-ice composition may be implausible for cryomagmatic liquids [Ruesch et al., 2016a]. However, a pure-ice case is useful to consider as an end-member. In this case,

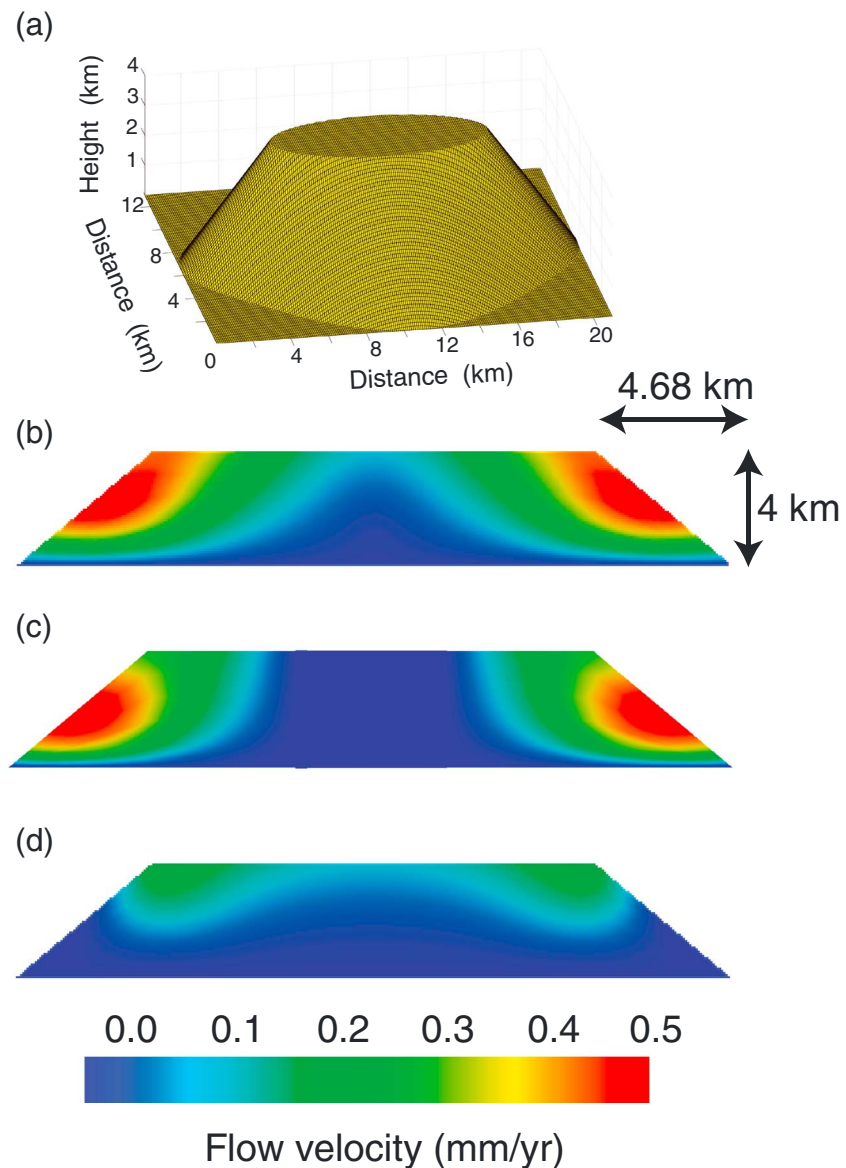


**Figure 3.** (a) FEM model of Ahuna Mons topography. We show 2-D east-west transects of (b) instantaneous total flow velocity, (c) instantaneous horizontal flow velocity, and (d) instantaneous vertical flow velocity. Positive horizontal/vertical directions are outward/down.

and when ice grain size is 1 mm, Ahuna Mons obtains flow velocities as high as 500 m/Myr with its present-day topography. The ice content needed for material to flow at all depends on the physical properties of the non-ice component, but past calculation of regolith dry packing density has estimated the minimum ice content to be 40% [Durham *et al.*, 2009]. At this minimum content, Ahuna Mons obtains flow velocities of 10 m/Myr with its present-day topography. Below this ice content, flow is negligible.

We consider the effects of uncertain physical parameters on our results. Because we are interested in application of our results to hypothetical cryovolcanic domes at other locations, in Figure 4a we show flow velocities for different temperatures (or equivalently, latitudes, Figure 2). We show velocities for temperatures as high as 160 K, the maximum annual-average temperature on Ceres, and as low as 100 K, below which flow is negligible over the age of the solar system, even in cases of pure ice. Study of ice rheology is ongoing, and the difference in velocities between using the rheology of Goldsby and Kohlstedt [2001] and that of Glen [1955] is approximately a factor of 2 (Figure 4a). The effects of ice content and ice grain size are quantified in Figure 4b, with ice content being the more sensitive parameter.

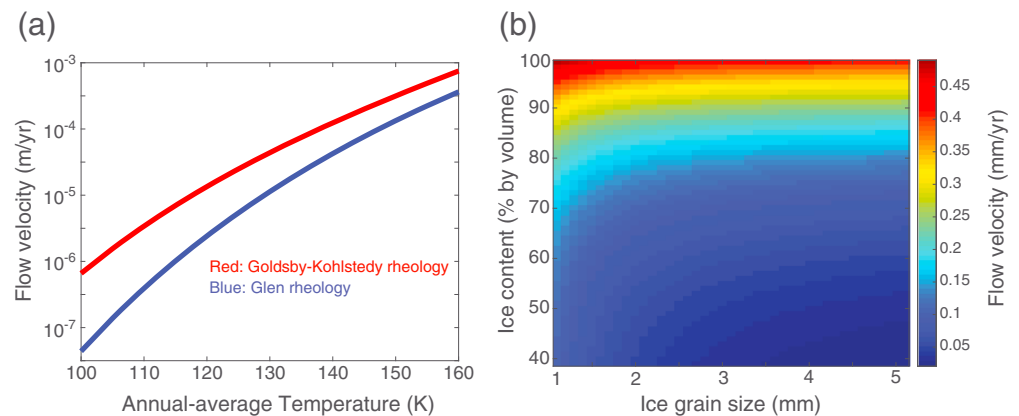


**Figure 4.** (a) Maximum flow velocity as a function of annual-average surface temperature for *Goldsby and Kohlstedt* [2001] and *Glen* [1955] rheologies. (b) Sensitivity of Ahuna Mons flow velocity (annual-average temperature 155 K) to volumetric ice content and ice grain size assumptions.

#### 4. Discussion

Our flow velocities of 10–500 m/Myr imply that Ahuna Mons, if sufficiently ice rich ( $> \sim 40\%$  volumetric ice content), will flow over geologically short timescales. Ahuna Mons is unlikely to be pure ice [*Ruesch et al.*, 2016a], and therefore we favor velocities at the slower end of the velocity range. Such speeds imply that Ahuna Mons will noticeably change its morphology over tens of million years. As the slopes of Ahuna Mons shallow, they will flow slower. Simulations that fully evolve the mountain through geologic time are further discussed below (Figure 3 shows instantaneous flow velocities at present day), but the models with the slowest allowable velocities cause the slopes of Ahuna Mons to shallow from  $40^\circ$  to an average of  $30^\circ$  over  $\sim 100$  Myr. These flow rates are sufficiently fast to subdue ice-rich cryovolcanic domes older than hundreds of million years (and perhaps tens of million years, depending on ice content) while not yet heavily affecting the geologically young Ahuna Mons. This result applies to hypothetical cryovolcanic domes at the low latitudes and midlatitudes of Ceres, but any polar domes [*Ruesch et al.*, 2016b] would experience lower temperatures and would not flow appreciably over geologic time.

If other features on Ceres are ancient cryovolcanic mounds, our models provide constraints on their ages. In aggregate, our models can thus provide volumetric constraints on the cryovolcanic history of Ceres. Assuming that cryovolcanic features have an initial state similar to Ahuna Mons (represented in idealized form in our model as a 4 km high mountain with  $40^\circ$  slopes), we ran FEM models forward in time to constrain their ages. Although mass wasting is hypothesized to be the source of Ahuna Mons' steep slopes, this process is part of the dome's initial emplacement and not continuously occurring after formation [*Ruesch et al.*, 2016a]. Under our hypothesis viscous flow is the primary factor controlling flank slopes over geologic time and will make those slopes shallower than the angle of repose, limiting the role of mass wasting in the future. Therefore, we estimate age as a function of aspect ratio under the assumption that a feature is sufficiently ice rich to flow in Figure 5. Results depend upon ice content and annual-average temperature (i.e., latitude). We include cases where domes are pure ice as an end-member constraint.

One application of the above ideas is to analyze another domal feature near the location of Ahuna Mons. The tholus unit mapped by *Ruesch et al.* [2016a] is a broad positive topographic feature underlying Ahuna Mons that is  $\sim 30$  km wide and  $\sim 2$  km high. The tholus is older than Ahuna Mons, but the presence of secondary crater chains makes crater size-frequency analysis difficult. *Ruesch et al.* [2016a] speculate that broader topographic rises such as the tholus may be extrusive domes that represent cryomagmas of different rheologies compared to Ahuna Mons. We instead suggest that the tholus represents a cryovolcanic unit originally similar to Ahuna Mons but viscously relaxed. If so, our models suggest an age between 25 and 500 Ma depending on ice content. As with Ahuna Mons, we consider previous work arguing that cryovolcanic units are unlikely to represent pure ice [*Ruesch et al.*, 2016a] and thus favor the older ages in this range.

Our hypothesis is only correct under the assumption that domes are sufficiently ice rich to experience significant viscous flow [*Durham et al.*, 2009]. Viscous flow shallows mountain slopes with age, so our hypothesis

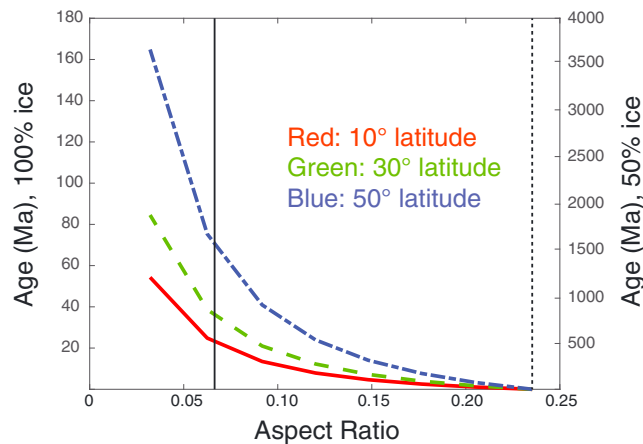


**Figure 5.** Estimated ages of hypothetical relaxed cryovolcanic domes as a function of their aspect ratio. Results are based on model runs evolving icy topography over time. Vertical dotted and solid lines show aspect ratios for Ahuna Mons ( $\sim 0.24$ ) and the underlying tholus ( $\sim 0.067$ ), respectively. Vertical axes show results for cases where domes are 100% (left) and 50% (right) ice by volume.

temperatures comparable to flat terrain at the pole, and an equatorward facing  $40^\circ$  slope has temperatures comparable to flat terrain at the equator. Temperature differences of this magnitude have large effects on flow velocity (Figure 4a). Therefore, cryovolcanic domes at midlatitudes should have detectable asymmetric shapes (with poleward facing slopes steeper than equatorward facing slopes) if they are tens of million years or older and sufficiently ice rich to experience flow. We ran a flow simulation for a half-ice dome with the dimensions of Ahuna Mons located at  $55^\circ\text{S}$  (where temperature differences between pole-facing and equator-facing slopes are maximized) instead of  $\sim 10^\circ\text{S}$  and found that it develops a  $10^\circ$  difference between north facing and south facing slopes in  $\sim 50$  Myr.

## 5. Conclusions

Viscous flow of topography is a modification mechanism that can describe the presence of a single, young, prominent cryovolcano (Ahuna Mons). Flow velocities are fast enough to heavily modify structures on time-scales of tens to hundreds of million years, shallowing their topographic relief and providing an explanation for why Dawn observations have not yet identified a plethora of cryovolcanoes. Flow velocities are not so fast that the observed near-pristine state of Ahuna Mons becomes problematic. Domes must be more compositionally ice rich than the average Cerean crust to flow, which is a reasonable property for a cryovolcanic construct. Our hypothesis works with any volumetric fraction of ice  $> \sim 40\%$ , but we favor the lower end of this range because past studies do not favor a pure-ice composition for Ahuna Mons. Cerean cryovolcanism involving cryomagma that is approximately half water by volume fits both Dawn observations and our FEM models. Based on our results, we predict that older cryovolcanoes have shallower slopes and that cryovolcanoes at midlatitudes have asymmetries between poleward and equatorward facing slopes. We do not expect extensive viscous relaxation of polar features. The detection of this distribution of features would add strong support to the hypothesis that Ceres undergoes ice-rich cryovolcanism, and flow models would constrain Cerean cryovolcanic history.

## References

- Aharonson, O., and N. Schorghofer (2006), Subsurface ice on Mars with rough topography, *J. Geophys. Res.*, *111*, E11007, doi:10.1029/2005JE002636.
- Bills, B. G., and B. R. Scott (2017), Secular obliquity variations of Ceres and Pallas, *Icarus*, *284*, 59–69.
- Bland, M. T. (2013), Predicted crater morphologies on Ceres: Probing internal structure and evolution, *Icarus*, *226*, 510–521.
- Bland, M. T., K. N. Singer, W. B. McKinnon, and P. M. Schenk (2012), Enceladus' extreme heat flux as revealed by its relaxed craters, *Geophys. Res. Lett.*, *39*, L17204, doi:10.1029/2012GL052736.
- Bland, M. T., et al. (2016), Composition and structure of the shallow subsurface of Ceres revealed by crater morphology, *Nat. Geosci.*, *9*, 538–542.
- Buczkowski, D. L., et al. (2016), The geomorphology of Ceres, *Science*, *353*, 1004.
- Castillo-Rogez, J. C. (2011), Ceres—Neither a porous nor salty ball, *Icarus*, *215*, 599–602.

could be tested by establishing a negative correlation between aspect ratio and ages from crater size-frequency analysis. Because of high uncertainties with this method, a more promising method is to search for topographic asymmetries of other dome-like features [Buczkowski et al., 2016] or tholi [Hughson et al., 2016]. At the low latitudes where Ahuna Mons resides, the effect of slope on annual-average temperature, and therefore flow velocity, is minimal. However, this effect is large at midlatitudes (maximized at  $\sim 55^\circ\text{S}$ , Figure 2), where surface slope of  $40^\circ$  causes temperature differences of tens of kelvins between poleward and equatorward orientations. At  $55^\circ$  latitude, a poleward facing  $40^\circ$  slope has

## Acknowledgments

The Dawn spacecraft data used in this study are publicly available in the NASA Planetary Data System (<https://pds.nasa.gov>). We thank two anonymous reviewers for their constructive remarks which improved the quality of the manuscript. We thank Simone Marchi for a helpful discussion regarding plausible compositions of Ahuna Mons. Any use of trade, firm, or product names is for descriptive purposes only and does not imply endorsement by the U.S. Government.

- Castillo-Rogez, J. C., and T. B. McCord (2010), Ceres' evolution and present state constrained by shape data, *Icarus*, *205*, 443–459.
- Castillo-Rogez, J. C., et al. (2016), Ceres' geophysical evolution inferred from Dawn data, AAS/Division for Planet. Sci. No. 48.
- Combe, J.-P., et al. (2016), Detection of local H<sub>2</sub>O exposed at the surface of Ceres, *Science*, *353*, 1007.
- Dombard, A. J., and W. B. McKinnon (2006), Elastoviscoplastic relaxation of impact crater topography with application to Ganymede and Callisto, *J. Geophys. Res.*, *111*, E01001, doi:10.1029/2005JE002445.
- Durham, W. B., and L. A. Stern (2001), Rheological properties of water ice—Applications to satellites of the outer planets, *Annu. Rev. Earth Planet. Sci.*, *29*, 295–330.
- Durham, W. B., S. H. Kirby, and L. A. Stern (1992), Effects of dispersed particulates on the rheology of water ice at planetary conditions, *J. Geophys. Res.*, *97*, 20,883–20,897, doi:10.1029/92JE02326.
- Durham, W. B., A. V. Pathare, L. A. Stern, and H. J. Lenferink (2009), Mobility of icy sand packs, with application to Martian permafrost, *Geophys. Res. Lett.*, *36*, L23203, doi:10.1029/2009GL040392.
- Ermakov, A. I., M. T. Zuber, D. E. Smith, R. R. Fu, C. A. Raymond, R. S. Park, and C. T. Russell (2016a), Evaluation of Ceres' compensation state, LPSC 47th, pp. 1708.
- Ermakov, A. I., E. Mazarico, S. Schroeder, U. Carsenty, N. Schorghofer, C. A. Raymond, and M. T. Zuber (2016b), Ceres' obliquity history: Implications for permanently shadowed regions, AGU Fall Meeting, P43C-2126.
- Fink, J. H., and N. T. Bridges (1995), Effects of eruption history and cooling rate on lava dome growth, *Bull. Volcanol.*, *57*, 229–239.
- Fu, R. R., A. I. Ermakov, S. Marchi, J. C. Castillo-Rogez, C. A. Raymond, S. D. King, M. T. Bland, and C. T. Russell (2016), Thermal evolution and fluid flow in planetesimals inferred from Dawn mission observations of Ceres, *79th Met. Soc.*, pp. 6107.
- Gagliardini, O., et al. (2013), Capabilities and performance of Elmer/Ice, a new-generation ice sheet model, *Geosci. Model Dev.*, *6*, 1299–1318.
- Glen, J. W. (1955), The creep of polycrystalline ice, *Proc. R. Soc. London, Ser. A*, *228*, 519–538.
- Goldsby, D. L., and D. L. Kohlstedt (2001), Superplastic deformation of ice: Experimental observations, *J. Geophys. Res.*, *106*, 11,017–11,030, doi:10.1029/2000JB900336.
- Hayne, P. O., and O. Aharonson (2015), Thermal stability of ice on Ceres with rough topography, *J. Geophys. Res. Planets*, *120*, 1567–1584, doi:10.1002/2015JE004887.
- Hiesinger, H., et al. (2016), Cratering on Ceres: Implications for its crust and evolution, *Science*, *353*, 1003.
- Hughson, K., et al. (2016), Geological mapping of the Ac-H-5 Fejokoo quadrangle of Ceres from NASA's Dawn mission, EGU Gen. Ass., 5022.
- Kargel, J. S. (1991), Brine volcanism and the interior structures of asteroids and icy satellites, *Icarus*, *94*, 368–390.
- Krohn, K., et al. (2016), Cryogenic flow features on Ceres: Implications for crater-related cryovolcanism, *Geophys. Res. Lett.*, *43*, 11,994–12,003, doi:10.1002/2016GL070370.
- Lopes, R. M. C., et al. (2007), Cryovolcanic features on Titan's surface as revealed by the Cassini Titan Radar Mapper, *Icarus*, *186*, 395–412.
- McCord, T. B., and C. Sotin (2005), Ceres: Evolution and current state, *J. Geophys. Res.*, *110*, E05009, doi:10.1029/2004JE002244.
- Miyamoto, H., G. Mitri, A. P. Showman, and J. M. Dohm (2005), Putative ice flows on Europa: Geometric patterns and relation to topography collectively constrain material properties and effusion rates, *Icarus*, *177*, 413–424.
- Moore, J. M., et al. (2016), The geology of Pluto and Charon through the eyes of New Horizons, *Science*, *351*, 1284.
- Park, R. S., et al. (2016), A partially differentiated interior for (1) Ceres deduced from its gravity field and shape, *Nature*, *537*, 515–517.
- Pathare, A. V., and D. A. Paige (2005), The effects of Martian orbital variations upon the sublimation and relaxation of north polar troughs and scarps, *Icarus*, *174*, 419–443.
- Quick, L. C., L. S. Glaze, and S. M. Baloga (2017), Cryovolcanic emplacement of domes on Europa, *Icarus*, *284*, 477–488.
- Ruesch, O., et al. (2016a), Cryovolcanism on Ceres, *Science*, *353*, 1005.
- Ruesch, O., et al. (2016b), Geology of Ceres' north polar quadrangle with Dawn FC imaging data, EGU Gen. Ass., 10455.
- Russell, C. T., et al. (2016), Dawn arrives at Ceres: Exploration of a small, volatile-rich world, *Science*, *353*, 1008–1010.
- Schmidt, B. S., et al. (2016), Icing in the cake: Evidence for ground ice in Ceres, AAS/Division for Planet. Sci. 48.
- Sori, M. M., S. Byrne, C. W. Hamilton, and M. E. Landis (2016), Viscous flow rates of icy topography on the north polar layered deposits of Mars, *Geophys. Res. Lett.*, *43*, 541–549, doi:10.1002/2015GL067298.
- Thomas, P. C., J. W. Parker, L. A. McFadden, C. T. Russell, S. A. Stern, M. V. Sykes, and E. F. Young (2005), Differentiation of the asteroid Ceres as revealed by its shape, *Nature*, *437*, 224–226.
- Voight, B., and D. Elsworth (1997), Failure of volcano slopes, *Geotechnique*, *47*, 1–31.
- Zambon, F., et al. (2016), Spectral analysis of Ahuna Mons from Dawn mission's visible-infrared spectrometer, *Geophys. Res. Lett.*, *43*, L71303, doi:10.1002/2016GL071303.
- Zolotov, M. Y. (2009), On the composition and differentiation of Ceres, *Icarus*, *204*, 183–193.